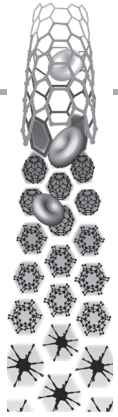

Development of screening assays for nanoparticle toxicity assessment in human blood: preliminary studies with charged Au nanoparticles

As nanoparticles have found increased use in both consumer and medical applications, corresponding increases in possible exposure to humans necessitate studies examining the impacts of these nanomaterials in biological systems. This article examines the effects of approximately 30-nm-diameter gold nanoparticles, with positively and negatively charged surface coatings in human blood. Here, we study the exposure effects, with up to 72 h of exposure to 5, 15, 25 and 50 µg/ml nanoparticles on hemolysis, reactive oxygen species (ROS) generation and platelet aggregation in subsets of cells from human blood. Assessing viability with hemolysis, results show significant changes in a concentration-dependent fashion. Rates of ROS generation were investigated using the dichlorofluorscein diacetate-based assay as ROS generation is a commonly suspected mechanism of nanoparticle toxicity; herein, ROS was not a significant factor. Optical monitoring of platelet aggregation revealed that none of the examined nanoparticles induced aggregation upon short-term exposure.

Original submitted 13 October 2011; Revised submitted 16 January 2012; Published online 14 May 2012

KEYWORDS: gold ■ hemolysis ■ nanoparticle ■ platelet aggregation ■ reactive oxygen species

Sara A Love[1], John W Thompson[1] & Christy L Haynes*[1]

[1]Department of Chemistry, University of Minnesota, Kolthoff & Smith Halls, 207 Pleasant Street SE, Minneapolis, MN 55455, USA
**Author for correspondence: chaynes@umn.edu*

The recent boom in nanotechnology has been staggering – as of March 2011, the number of consumer products containing nanoparticles (1317) is over 24-times that of what it was in 2005 [101]. Consumer products alone do not account for all of the US$251 billion industry, which is expected to grow to over $2.4 trillion by 2015 with nanomedicines also making up a significant portion [1]. There are already several US FDA-approved nanomedicines, and this type of medicine has become the primary treatment for certain neoplastic conditions [2–4]. One nanomaterial in particular that has exhibited much recent growth in both the consumer and medical fields is nanoscale Au. With the number of Au nanomaterial-containing consumer product (lines) going from zero to 28 between 2005 and 2010, and the exploration of various applications for Au nanoparticle-based cancer treatment in the medical field, Au nanomaterials have certainly become a rapidly expanding area of investigation [5–9,101].

If nanoparticle exposure does occur, either intentionally or unintentionally, there is a good probability that these nanoparticles will interact with blood cells. As such, *in vitro* toxicity evaluations with blood cells provide an excellent model system for human cell nanotoxicity studies. In addition, the use of primary human cells isolated directly from blood minimizes the common complication of poor correlation between *in vitro* and *in vivo* studies [10]. In recent years, nanoparticle toxicity studies have been performed using a variety of cell types, including cells isolated from the blood [11–15]. The composition of blood is complex and consists of three main cell-(like) fractions, red blood cells (RBCs), white blood cells (WBCs) and platelets. Each of these components play a critical role in overall health and blood hemostasis, specifically oxygen transport (RBCs), immune response (WBCs) and clot formation (platelets) and, is therefore, critically important to maintaining a normal physiological response, even upon exposure to nanoparticles.

Recent studies have examined the impact of several types of nanoparticles on RBC hemolysis [13,14,16,17]. While hemolysis provides viability information, cells either remain intact or they are lysed upon exposure, and the use of additional 'functional' studies improves on the overall understanding of potential mechanisms of toxicity. Therefore, it is only by examining other cell populations with more mechanistic studies that one can assess wider toxicity implications of nanoparticle exposure. Recent nanotoxicity studies have shown that a probable mechanism of nanoparticle toxicity is the induction of oxidative stress or altered/increased production of reactive oxygen species (ROS) [18–20]. ROS, if

Future Medicine part of fsg

unchecked, can cause widespread changes to cells including oxidation of proteins, lipids and DNA that can alter cell function and potentially cause cell death. Oxidative stress is known to have deleterious effects and has been shown to be a potential factor in aging and a variety of diseases such as Parkinson's and cancer [21–23]. Cells have numerous mechanisms in place to manage ROS, including enzymatic breakdown pathways (e.g., superoxide dismutase or catalase). Typically, molecular ROS generation is monitored by fluorescence assays using exogenous substrates that fluoresce upon interaction with ROS such as with 2′,7′-dichlorofluorscein diacetate (DCFDA), or by monitoring the levels and oxidation state of glutathione, a tripeptide key to maintaining the cellular redox state [19,21]. WBCs, primarily neutrophils (~50–70% of WBCs), are a subset of phagocytic cells responsible for oxidative breakdown of possible pathogens; they are therefore an ideal population of blood cells for examination of ROS generation in response to nanoparticle exposure. While considered a probable mechanism of nanoparticle toxicity, there are numerous possible mechanisms of functional alteration that could be equally or more deleterious to cells.

Another major fraction of blood is the plasma, containing platelets, the cell-like bodies responsible for clot formation. As the role of platelets in clot formation is critical to maintaining normal blood hemostasis, monitoring platelet activation (and thus clot formation) upon nanoparticle exposure is a functional indicator of possible toxicity [24–26]. Clot formation *in vivo* must be tightly controlled as both increased and decreased clot formation can have deleterious effects; this assessment can reveal insight into the pro- and antithrombotic activity of nanoparticle exposure.

Here, we report our investigation of the effects of the Au nanoparticle (with ~30 nm diameter and varied ζ-potential) exposure on RBC hemolysis, ROS generation in WBCs and platelet aggregation. By examining these three components, we expand the current understanding of Au nanoparticle toxicity within human blood. In addition, we can compare these human cell toxicity findings to previous work with these nanoparticles in murine mast cells to assess the potential toxic effects of nanoparticles across species and cell types [2].

Materials & methods

Reagents & chemicals

Unless otherwise stated, chemicals utilized were purchased from Sigma Aldrich (WI, USA) and used without additional purification. All blood was drawn and collected in heparin sodium vacuum tubes at Memorial Blood Center (MN, USA). Water used in synthesis was purified using a Milli-Q® Integral Water Purification System (Millipore, MA, USA).

Nanoparticle synthesis

All nanoparticles were synthesized using previously published methods [2]. All glassware used was cleaned with aqua regia (3:1 concentrated HCl:HNO_3) and thoroughly rinsed prior to synthesis. First, the particles designated 'seed Au' were prepared in the following manner: 240 µl of approximately 30% by weight $HAuCl_4$ solution was added to 400 ml of Milli-Q water (Millipore, MA, USA); 40 ml of a 1% by weight trisodium citrate solution was added under rapid stirring; the solution was sonicated at 37°C under N_2 for 30 min (during which time the solution turned from a pale gold color to dark violet); and the nanoparticle solution was centrifuged (Optima™ L-100k Ultracentrifuge, Beckman Coulter, CA, USA) and washed twice at 28,627 × g for 15 min. Second, the particles designated 'Au(+)' and 'Au(-)' were synthesized by adjusting the seed Au solution to pH 11 with NaOH and adding 100 µl of 10 mM α-lipoic acid in ethanol per ml of seed Au solution under rapid stirring. This solution was then stirred overnight (~12–18 h) and centrifuged at 28,627 × g for 15 min. After centrifugation, the nanoparticles were washed with water and 100 µl of either 10 mM 11-mercaptoundecanoic acid in ethanol or 4 mM 11-mercaptoundecylamine in ethanol was added per ml of solution, depending on whether negative or positive Au, respectively, was desired. After addition of 11-mercaptoundecanoic acid, the solution was again allowed to stir overnight (~12–18 h); however, 1 h after the addition of 11-mercaptoundecylamine, 100 µl of 1 M HCl was added per ml of solution and then allowed to stir overnight. To purify the nanoparticles after synthesis and ligand exchange, both nanoparticle solutions were centrifuged (28,627 × g for 15 min) and washed twice with H_2O to eliminate noncovalently bound ligand. The final pellet was resuspended in H_2O and the nanoparticles were characterized using a variety of methods.

Characterization

The synthesized nanoparticles were characterized by transmission electron microscopy (TEM) after dispersion on formvar-coated grids (Ted Pella, CA, USA) using JEOL®

1200EX (Tokyo, Japan) at an accelerating voltage of 120 kV. Size was determined using ImageJ™ software (NIH, MD, USA) based on the average of at least 200 individual nanoparticle measurements. Hydrodynamic diameter, both in the original solution (water) and 10% bovine calf serum, was measured by dynamic light scattering using a ZetaPALS™ instrument (Brookhaven Instruments, NY, USA) and expressed as an average of three 1 min measurements. Extinction measurements were conducted using an Ocean Optics® USB 2000 spectrometer (FL, USA) as a secondary examination of nanoparticle aggregation state. All nanoparticle concentrations were assessed by inductively coupled plasma atomic emission spectroscopy to determine total ionic Au content upon complete nanoparticle dissolution (Optima™ 3000DV, Perkin Elmer, MA, USA) and were then diluted, as needed (stock concentrations of 139 ± 51, 160 ± 77, and 123 ± 44 µg/ml for seed, Au[+] and Au[-], respectively), to the reported exposure concentrations (between 5 and 50 µg/ml). This dosing range was chosen to represent the range from lower/unintentional (i.e., release into the environment) to higher/intentional exposure levels (i.e., therapeutics). The exposure time frames were chosen to focus on short-term (i.e., 5 min, depending on cell limitations) or repeat/multiple exposure (up to 72 h) likely to be encountered in either accidental or therapeutic settings, respectively. All nanoparticles were stored in the dark or under minimal light exposure prior to and during cell incubation.

Hemolysis

RBCs were isolated according to a modified version of the method employed by Lin and Haynes [14]. Briefly, a 5 ml blood sample was mixed with 10 ml of phosphate-buffered saline (PBS) lacking calcium and magnesium (PBSd) and centrifuged at 10,016 × g for 5 min. The supernatant was drawn off and five subsequent washes were carried out before diluting the sample to a final volume of 50 ml in PBSd. The RBCs were then diluted 1:5 into: PBSd (negative control); water (positive control); or a nanoparticle solution (in PBSd) at varying concentrations/types (experimental conditions) in triplicate, repeated with at least three separate blood samples (donors). The negative control was composed of PBSd with water at the same volume as the largest volume of the nanoparticle solution, while the positive control was only water to ensure complete release of hemoglobin from all the RBCs via osmotic cell lysis. The samples were left at room temperature in the dark for 24 h and then centrifuged at 10,016 × g for 3 min. After centrifuging, the supernatant was transferred to a 96-well plate and the absorbance at 570 nm was recorded. Additional assessments were made over 72 h of exposure, at 24-h intervals. Percent hemolysis was calculated using Equation 1:

$$Hemolysis\,(\%\ of\ positive\ control) = 100\left(\frac{Abs_{sample} - Abs_{neg}}{Abs_{pos} - Abs_{neg}}\right) \quad (1)$$

ROS generation

Neutrophils were isolated from human blood following the methods of Bass *et al.* [27]. Briefly, heparinized blood was layered over Ficoll Plaque Plus© (GE Healthcare, NJ, USA) and allowed to separate by gravity for approximately 1 h. The leukocyte-rich supernatant was then drawn off, layered over Ficoll Plaque Plus, and centrifuged at 400 × g for 40 min. The neutrophil-containing pellet was then washed three-times with PBS containing glucose but lacking calcium and magnesium (PBSg), and resuspended at a cell density of 1×10^6 cells/ml. ROS generation was then measured using a DCFDA-based spectroflurometric assay. For this assay, 80 µl of the neutrophil solution was transferred to a 96-well plate where it was mixed with 20 µl of 100 µM DCFDA, varying amounts of nanoparticle solutions, and finally, enough PBSg to bring the total volume in each well to 200 µl. The negative control was prepared in the same manner but replacing the nanoparticle solution with PBSg. Two different positive controls were prepared: one exposed to UV light (at 365 nm with an irradiance of 14.5 J m^{-2}) for the duration of the exposure, and the other was exposed to 1 unit/ml of thrombin for the duration of the assay. Each condition was carried out in eight replicates and was performed with at least three independent blood samples. Emission readings ($\lambda_{excitation}$ = 485 nm, $\lambda_{emission}$ = 528 nm) were taken on a Biotek Synergy 2™ microplate reader (Biotek, VT, USA) initially and again at 1, 2, 3 and 4 h after nanoparticle addition. Linear regression analysis (Microsoft Excel®, WA, USA) was then performed to determine the rate of ROS generation for each control and experimental condition. These rates were then compared using the Student's t-test to assess significant differences from the rate of generation for the negative-control condition.

Platelet aggregation

Platelets were isolated from whole human blood following the platelet separation described by Chrono-log Instruments (Chrono-log, PA, USA) [28]. Briefly, whole blood was centrifuged for 15 min at 100 × g. The platelet-rich plasma (PRP) was then drawn off and stored at room temperature for the remainder of the assay. The PRP needed for individual trials was placed in a heating block warmed to a temperature of 37°C. A small volume of PRP was then centrifuged at 2400 × g for 20 min to obtain platelet-poor plasma (PPP) for use as a blank. After centrifugation, the PPP was warmed to 37°C and placed in the blank channel of the aggregometer (Chrono-log) for the remainder of the assay. Once the temperature of the PRP for each trial had reached 37°C, it was placed into the aggregometer using PPP as a blank. The following trials were then performed while stirring vigorously (1000 rpm): 100 µl of PBSg (negative control); thrombin and ADP with a final concentration of 1 unit/ml and 40 µM, respectively (positive control); and varying concentrations/types of nanoparticles. All trials were allowed to proceed for 5 min or until 100% aggregation had been achieved; for all conditions, statistical significance was assessed by analysis of variance (ANOVA) with a Dunnett's post-test to compare the experimental conditions with the negative control ($p < 0.05$; Prism®, GraphPad software, CA, USA).

Results & discussion

Nanoparticle synthesis & characterization

Spherical Au nanoparticles of approximately 30-nm diameter and of varying ζ-potential were synthesized, as shown in Figure 1. The average nanoparticle diameter, measured via TEM, was determined to be 26.5 ± 4.0 nm for the seed Au, 25.2 ± 4.7 nm for Au(+) and 26.9 ± 7.6 nm for Au(-); nanoparticle characteristics are summarized in Figure 1. As in related studies [2], these nanoparticles have diameters known to be within the regime of maximal uptake into mammalian cells [29]. Purified nanoparticles were examined using dynamic light scattering over 3 days to determine nanoparticle stability in PBSd with 10% bovine calf serum, the dosing vehicle. All three nanoparticles were found to have consistent hydrodynamic radii over the 72 h exposure period, shown in Supplementary Figure 1 (see online at www.futuremedicine.com/doi/suppl/10.2217/NNM.12.17). While uptake of these nanoparticles was not explicitly examined here, previous studies have found that nanoparticles interact with blood cells and can be internalized, such as in TEM studies with RBCs [30,31]. In addition, previous work by Marquis *et al.* found that these nanoparticles were taken up in a concentration-dependent fashion (tested up to 15 µg/ml) and were taken into murine mast cells at similar rates for positively and negatively charged nanoparticles [2].

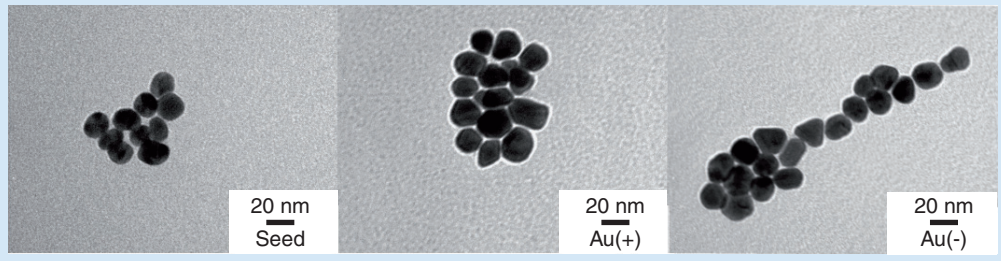

Nanoparticle	Diameter (by TEM, nm)	LSPR (I_{max}, nm)	z potential (mV)
Seed	26.5 ± 4.0	525.4	-41.0 ± 1.2
Au(+)	25.2 ± 4.7	529.6	41.9 ± 1.3
Au(-)	26.9 ± 7.6	529.6	-39.4 ± 1.8

Figure 1. Representative transmission electron microscopy images of seed, Au(+) and Au(-) nanoparticles with table of associated nanoparticle parameters.
LSPR: Localized surface plasmon resonance; TEM: Transmission electron microscopy.

Hemolysis

RBC hemolysis was calculated based on the measured absorbance due to free hemoglobin relative to total hemoglobin from complete cell lysis, in triplicate samples from at least three separate blood samples (donors). As Au nanoparticle extinction is typically found near the absorbance for hemoglobin, a simple test of Rayleigh scattering from the nanoparticles in blood samples was evaluated, as shown in Supplementary Figure 2, comparing centrifuged and uncentrifuged samples following exposure to nanoparticles. These were found to show scattering, indicative of nanoparticle presence, in only the uncentrifuged sample (Supplementary Figure 2). This scattering indicates that the measured absorbance in the tested supernatant was due to the presence of free hemoglobin and not any remaining suspended nanoparticles. Hemolysis was seen for each of the three examined nanoparticles as shown in Figure 2A–C (for seed Au, Au(-) and Au(+), respectively) at different concentrations. At 50 µg/ml, for all three nanoparticles, RBCs were found to undergo significant hemolysis of 77, 32 and 51% (where complete hemolysis was normalized to 100%) for seed, positive and negative Au, respectively, at 24 h (by ANOVA with a Dunnett's post-test to assess significant difference from the negative control; $p < 0.05$). The Au(-) nanoparticles also showed between 16 and 20% hemolysis at concentrations of 25 µg/ml and greater, while the Au(+) nanoparticles showed hemolysis (20% or more) at concentrations of 15 µg/ml and greater. In general, there appears to be a trend towards concentration-dependent hemolysis, most clearly seen in the case of Au(+) at 24 h of exposure (Figure 2D), but this trend occurs at different rates for each of the examined nanoparticles. Another interesting aspect of these results is

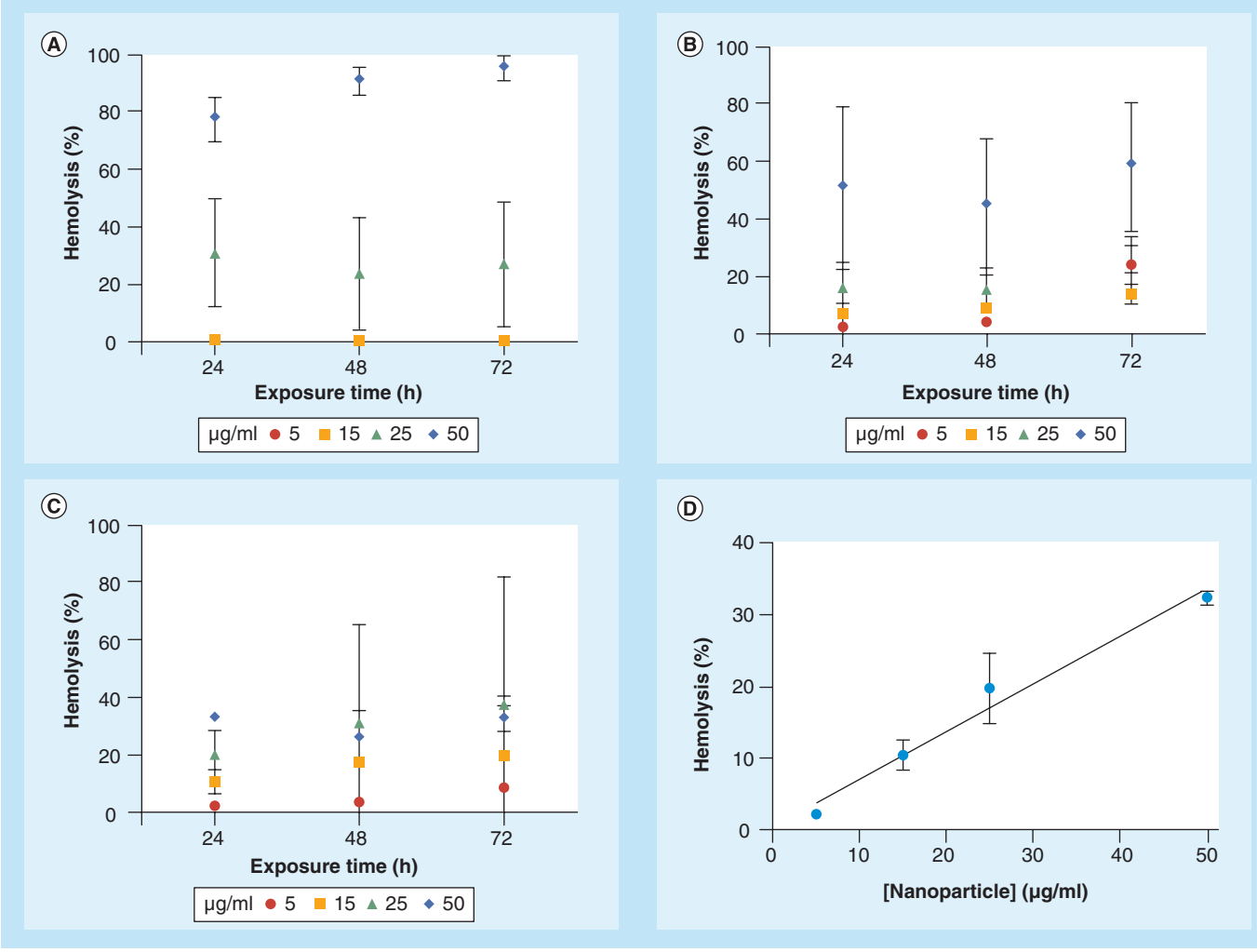

Figure 2. Hemolysis results reported as a percentage of the positive control condition. The higher hemolysis indicates higher levels of cell lysis and subsequent hemoglobin release for **(A)** seed, **(B)** Au(-), **(C)** Au(+) and **(D)** concentration-dependent trend in hemolysis as shown for 24 h of Au(+) exposure.

that two nanoparticles, with similar original size and ζ-potential, have different levels of induced hemolysis (77 vs 50%, seed vs Au[-], respectively). Despite being so similar at the time of synthesis, prior to serum exposure, there are differences in the hydrodynamic radius for these particles (Supplementary Figure 1). As recent work from the Dawson group and others suggests, there are probably differences in serum protein adsorption on the examined nanoparticles, driven by different surface functional groups [32–35]. Therefore, the observed differences in hemolysis could be due to the differences in the surface-adsorbed proteins themselves or from changes in the physiochemical properties of the nanoparticles upon differential serum protein adsorption. As with a similar previous study, Au(+) nanoparticles induced hemolysis at lower concentrations than negatively charged Au did, probably through passive membrane association [11]. These results are also in agreement with the results of Marquis *et al.*, examining murine mast cells with the same nanoparticles utilized here, having found that viability was decreased for the Au(+) at 15 μg/ml (their highest concentration tested) but not for Au(-) [2]. In another recent study, Schaeublin *et al.* examined approximately 2-nm Au with varied surface charge in human keratinocytes; their findings similarly showed dose-dependent effects and charged Au nanoparticles were more cytotoxic to cells then neutral Au [36]. Overall, the reported results suggest that there are unique interactions between the three nanoparticles examined and RBCs, owing to the differences in the ζ-potential and/or surface functional groups.

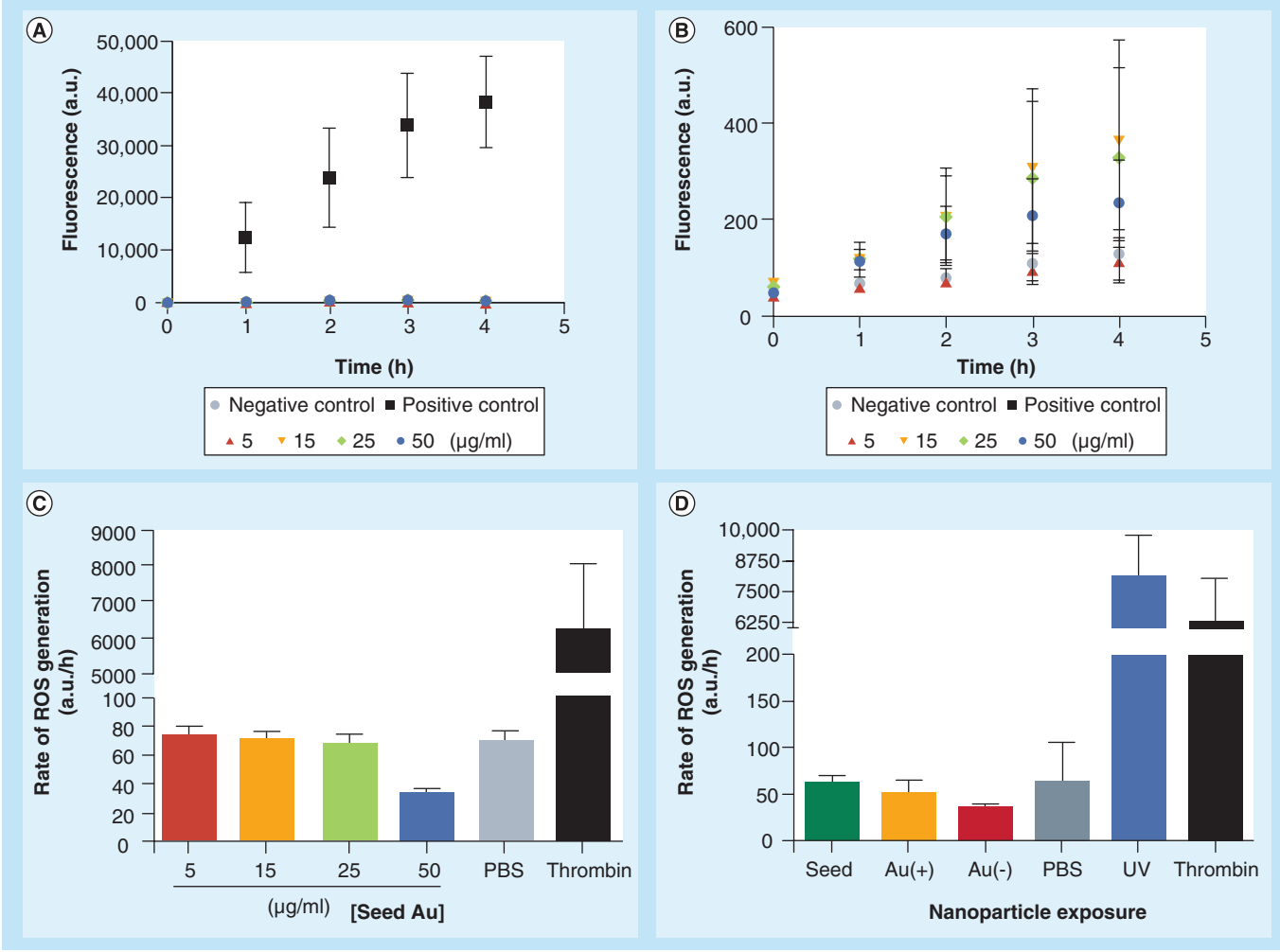

Figure 3. Rate of reactive oxygen species generation was not significantly different after exposure to seed, Au(+) and Au(-). (A) Au(+) ROS generation where the baseline area is enlarged in **(B)** to show that there is no significant difference for nanoparticle exposure from the negative control condition. **(C)** Rates of ROS generation for seed Au, where no significant ROS was generated. **(D)** The average rate of ROS generation for each of the three types of nanoparticles (seed, Au and PBS) as compared to both positive (UV and thrombin) controls.
PBS: Phosphate-buffered saline; ROS: Reactive oxygen species.

ROS generation

ROS is widely considered to be one of the probable mechanisms of nanoparticle toxicity, seen with various cells types and nanoparticles [18–20]. While this is only one possible mechanism to induce deleterious cellular effects upon nanoparticle exposure, ROS perturbations within blood could potentially compromise larger processes, such as inflammation or the immune response. Therefore, this potential mechanism of nanoparticle toxicity was studied by examining the rate of ROS generation in the WBC fraction, containing mainly neutrophils, as determined by the DCFDA assay. The DCFDA assay is considered to be promiscuous, thus allowing multiple forms of ROS, including superoxide and hydroxyl radical, to be assessed simultaneously. Owing to the short lifetime of primary culture neutrophils, approximately 6 h in cell culture, ROS generation was examined for up to 4 h of exposure to ensure measurements assessed nanoparticle exposure effects instead of cell death effects. Initially, and at hour time points, fluorescence was measured, and the average rate of ROS production was compared with controls. As these cells do not adhere sufficiently to cell culture dishes to allow cells to be thoroughly washed, the rate of ROS generation was examined to account for any remaining free extracellular DCFDA. Fluorescence was measured for a minimum of eight replicate wells using at least three separate blood samples (donors). As shown for Au(+)-exposed cells in Figure 3A, the average fluorescence measured was not found to be significantly different than cells unexposed to nanoparticles (as shown in the expanded baseline from A in B, these are typical of results for all exposure conditions). The average rate of ROS formation for all tested nanoparticles and concentrations were found to exhibit no significant changes in the rate of ROS generation when compared with the unexposed (negative) control, using ANOVA (with Dunnett's post-test) after the initial linear regression ($p > 0.05$). Typical rate results are shown in Figure 3C (seed Au), and the average rate of ROS generation for each nanoparticle type is shown in Figure 3D. Recent work suggests that ROS generation is dependent on surface functionalization [37,38], with changes in chemistry resulting in altered ROS generation (i.e., increased hydrophobicity resulting in increased ROS generation) [39]. However, the results reported here suggest that the mechanism of toxicity for these nanoparticles is probably unrelated to changes in oxidative stress, which is in agreement with studies in other cell types using these charged nanoparticles [2].

Platelet aggregation

Platelets are cell-like bodies that become activated and then aggregate, a key process in thrombosis. The aggregation state of platelets is one mechanism to measure their activation and can be done with a simple optical turbidity measurement, where transmittance increases as the platelets aggregate and fall out of suspension. Platelet aggregation was measured with at least four replicates from at least three separate blood samples (donors). For simplicity, Figure 4A shows a representative time course for the PBS exposed (negative control), ADP and thrombin exposed (positive control) and Au(+) at 15 µg/ml exposed conditions. Each trace is slightly offset for clarity and the arrows indicate when samples were added to the warmed, stirring platelet solutions. For short-term exposure (less than 20 min), none of the tested nanoparticles or doses induced significant platelet aggregation ($p > 0.05$), as summarized in Figure 4B, while the negative control had an average aggregation of 2.25 ± 1.43% (data not shown). The levels of aggregation at all examined conditions were not significantly different compared with the negative control or other nanoparticle-exposed conditions ($p > 0.05$). One study by Dobrovolskaia *et al.*, examined serum protein adsorption on citrate Au nanoparticles and found that these changes did not lead to altered platelet activation or aggregation, similar to the results reported herein [40]. These results differ from results found in a previous study where platelet aggregation was observed via microscopic examination [15]; however, differences in the Au nanoparticles and platelet handling (suspension vs adherent) could account for these divergent results. Typically, platelets are activated, and therefore aggregated, by negative surfaces; alternately, these results suggest that a negative ζ-potential is insufficient to induce activation/aggregation. These data indicate that there is either a critical threshold for contact that must be met to induce aggregation or that adsorption of serum proteins offsets the negative ζ-potential. These results could support a critical threshold for contact, a possible key concept in nanoparticle toxicity, and is similar to conclusions reached in recent work finding that surface contact was critical to modulating toxicity in the case of mesoporous silica [14].

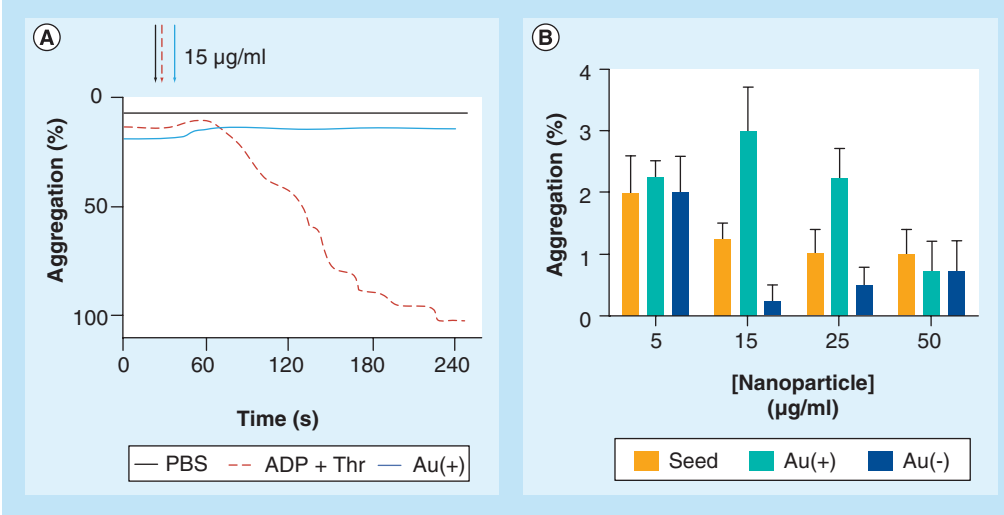

Figure 4. Platelet aggregation was not induced upon exposure to seed, Au(+) and Au(-). **(A)** Representative aggregation traces showing ADP/thrombin induced aggregation (+ control), PBS (- control) and nanoparticle exposure (Au[+] at 15 µg/ml), where no significant aggregation was caused by nanoparticle exposure and arrows indicate when nanoparticles or controls were added to the stirring platelet suspension. **(B)** A summary for the average nanoparticle-induced aggregation, none of which were significantly different from the negative control (not shown, average aggregation of 2.25 ± 1.43%) or the other nanoparticle-exposed conditions.
PBS: Phosphate-buffered saline; Thr: Thrombin.

Conclusion

To summarize this work, we have examined the effects of short-term nanoparticle exposure on cells isolated from human blood, at doses from 5 to 50 µg/ml with a combination of viability and functional assessments. Using hemolysis as a measure of cellular viability, exposure to Au(+) lead to increases in cell lysis in a concentration-dependent fashion above 15 µg/ml, while higher concentrations were needed for Au(-) (25 µg/ml) and seed Au (50 µg/ml) nanoparticles. While both the Au(-) and seed Au have very similar negative ζ-potentials, they showed different hemolytic capacity, indicating a more complex hemolysis interaction than nanoparticle ζ-potential differences would explain. As seen with other noble metal nanoparticles [2,39], these nanoparticles did not induce changes in ROS generation, despite recently reported findings that other nanoparticle compositions alter ROS generation and potentially explain observed nanotoxicity [19,36,37,41]. In addition, this work suggests that similar effects can be seen with diverse cells using consistent nanoparticles, exposure and dosing metrics. None of the examined nanoparticles induced platelet aggregation upon short-term exposure, suggesting that nonspecific aggregation owing to surface charge is not an activating factor for platelets. Finally, these studies (as described) provide an assessment method that readily examines nanoparticle toxicity with both viability and functional assessments, which can be adapted to examine synergistic effects by examining whole, instead of separated, blood components.

Future perspective

While there are numerous avenues of further research to pursue in this fashion, several interesting follow-up studies are directly indicated from the work presented herein. In this work, we have examined multiple cell populations from human blood separately to assess the possible toxicity of nanoparticles. As this approach readily lends itself to studies using whole blood, one further avenue to be pursued is assessment of nanoparticle exposure within whole blood, instead of within separated subpopulations, to examine any synergistic effects within these blood cell subpopulations. Beyond moving into studies with whole blood exposure, another avenue to examine is the effect of nanoparticle exposure with cells that have undergone some challenge prior to nanoparticle exposure. For example, one may assess the modulation of the platelet aggregation response after nanoparticle exposure in previously activated platelets (with agonists at subthreshold levels) to determine if nanoparticle exposure potentiates a normal hemostatic response. As the study described herein has focused on the effects of variations in one physiochemical property, further studies may examine additional properties such as

variations in the nanoparticle core composition (e.g., Ag and TiO_2), size or surface modification (e.g., polyethylene glycol passivation) to characterize modulation of the effects reported here. Finally, to better understand the observed toxicity described here, complimentary studies focusing on additional cellular functions (e.g., platelet exocytosis) may be conducted.

Financial & competing interests disclosure

This research was financially supported by a grant from the National Science Foundation (CHE-0645041), the Dreyfus Foundation and a University of Minnesota UROP for JW Thompson. The authors have no other relevant affiliations or financial involvement with any organization or entity with a financial interest in or financial conflict with the subject matter or materials discussed in the manuscript apart from those disclosed.

No writing assistance was utilized in the production of this manuscript.

Ethical conduct of research

The authors state that they have obtained appropriate institutional review board approval or have followed the principles outlined in the Declaration of Helsinki for all human or animal experimental investigations. In addition, for investigations involving human subjects, informed consent has been obtained from the participants involved.

Executive summary

Background

- Nanoparticle-exposure studies in human blood cells, using different cell populations, can provide insights into nanotoxicity.
- This work examines hemolysis, reactive oxygen species (ROS) generation, and platelet aggregation to assess cell viability and cellular functions after short-term exposure.

Results & discussion

- Spherical Au nanoparticles (~30-nm diameter) with varied ζ-potential were synthesized and characterized.
- After exposure, between 24 and 72 h, significant hemolysis was seen in a concentration-dependent manner.
- Rate of ROS generation was found not to be significantly different over 4 h of nanoparticle exposure, for all examined nanoparticles and concentrations.
- Platelet aggregation was not induced by exposure for all examined nanoparticles and concentrations.

Conclusion

- Hemolysis was induced in a concentration-dependent manner, above a unique concentration threshold for each Au nanoparticle examined.
- Hemolytic capacity was not dictated by the measured ζ-potential.
- Results here and elsewhere suggest that ROS is not a significant contributor to toxicity for these nanoparticles.
- None of the examined nanoparticles induced platelet aggregation.
- Negative ζ-potential was insufficient to induce platelet aggregation.

Future perspective

- Examine effects of nanoparticle exposure in whole blood, instead of separated cell populations.
- Examine effects of exposure with compromised or previously/partially activated cells.

References

1 Lux Research. *Nanomaterials State of the Market Q3 2008: Stealth Success, Broad Impact.* Lux Research, Inc., NY, USA (2008).

2 Marquis B, Liu Z, Braun K, Haynes C. Investigation of noble metal nanoparticle ζ-potential effects on single-cell exocytosis function *in vitro* with carbon-fiber microelectrode amperometry. *Analyst* 136(17), 3478–3486 (2011).

3 Dougherty T, Gomer C, Jori G. Photodynamic therapy. *J. Natl. Cancer Inst.* 90(12), 889–905 (1998).

4 Brown S, Brown E, Walker I. The present and future role of photodynamic therapy in cancer treatment. *Lancet Oncol.* 5(8), 497–508 (2004).

5 Chen J, Glaus C, Laforest R *et al.* Gold nanocages as photothermal transducers for cancer treatment. *Small* 6(7), 811–817 (2010).

6 Cheng Y, C Samia A, Meyers J *et al.* Highly efficient drug delivery with gold nanoparticle vectors for *in vivo* photodynamic therapy of cancer. *J. Am. Chem. Soc.* 130(32), 10643–10647 (2008).

7 Hone D, Walker P, Evans-Gowing R *et al.* Generation of cytotoxic singlet oxygen via phthalocyanine-stabilized gold nanoparticles: a potential delivery vehicle for photodynamic therapy. *Langmuir* 18(8), 2985–2987 (2002).

8 Wieder M, Hone D, Cook M *et al.* Intracellular photodynamic therapy with photosensitizer-nanoparticle conjugates: cancer therapy using a 'Trojan horse'. *Photochem. Photobiol. Sci.* 5(8), 727–734 (2006).

9 El-Sayed I, Huang X, El-Sayed M. Selective laser photo-thermal therapy of epithelial carcinoma using anti-EGFR antibody conjugated gold nanoparticles. *Cancer Lett.* 239(1), 129–135 (2006).

10 Sayes C, Reed K, Warheit D. Assessing toxicity of fine and nanoparticles: comparing *in vitro* measurements to *in vivo* pulmonary toxicity profiles. *Toxicol. Sci.* 97(1), 163–180 (2007).

11 Goodman C, McCusker C, Yilmaz T, Rotello V. Toxicity of gold nanoparticles functionalized with cationic and anionic side chains. *Bioconjug. Chem.* 15(4), 897–900 (2004).

12 Mayer A, Vadon M, Rinner B *et al.* The role of nanoparticle size in hemocompatibility. *Toxicology* 258(2–3), 139–147 (2009).

13 Liao K, Lin Y-S, Macosko C, Haynes C. Cytotoxicity of graphene oxide and graphene in human erythrocytes and skin fibroblasts. *ACS Appl. Mater. Interfaces* 3(7), 2607–2615 (2011).

14 Lin Y-S, Haynes C. Impacts of mesoporous silica nanoparticle size, pore ordering, and pore integrity on hemolytic activity. *J. Am. Chem. Soc.* 132(13), 4834–4842 (2010).

15 Wiwanitkit V, Sereemaspun A, Rojanathanes R. Gold nanoparticles and a microscopic view of platelets: a preliminary observation. *Cardiovasc. J. Afr.* 20(2), 141–142 (2009).

16 Ashokan A, Chandran P, Sadanandan A *et al.* Development and haematotoxicological evaluation of doped hydroxyapatite based multimodal nanocontrast agent for near-infrared, magnetic resonance and x-ray contrast imaging. *Nanotoxicology* 6, 652–666 (2012).

17 Choi J, Reipa V, Hitchins V, Goering P, Malinauskas R. Physicochemical characterization and *in vitro* hemolysis evaluation of silver nanoparticles. *Toxicol. Sci.* 123(1), 133–143 (2011).

18 Maurer-Jones M, Lin Y-S, Haynes C. Functional assessment of metal oxide nanoparticle toxicity in immune cells. *ACS Nano* 4(6), 3363–3373 (2010).

19 Wu J, Sun J, Xue Y. Involvement of JNK and P53 activation in G2/M cell cycle arrest and apoptosis induced by titanium dioxide nanoparticles in neuron cells. *Toxicol. Lett.* 199(3), 269–276 (2010).

20 Migdal C, Rahal R, Rubod A *et al.* Internalisation of hybrid titanium dioxide/para-amino benzoic acid nanoparticles in human dendritic cells did not induce toxicity and changes in their functions. *Toxicol. Lett.* 199(1), 34–42 (2010).

21 Gate L, Paul J, Ba G, Tew K, Tapiero H. Oxidative stress induced in pathologies: the role of antioxidants. *Biomed. Pharmacother.* 53(4), 169–180 (1999).

22 Orsucci D, Mancuso M, Lenco E, Logerfo A, Siciliano G. Targeting mitochondrial dysfunction and neurodegeneration by means of coenzyme Q10 and its analogues. *Curr. Med. Chem.* 18(26), 4053–4064 (2011).

23 Gupta A, Kumar A, Kulkarni S. Targeting oxidative stress, mitochondrial dysfunction and neuroinflammatory signaling by selective cyclooxygenase (COX)-2 inhibitors mitigates MPTP-induced neurotoxicity in mice. *Prog. Neuropsychopharmacol. Biol. Psych.* 35(4), 974–981 (2011).

24 Radomski A, Jurasz P, Alonso-Escolano D *et al.* Nanoparticle-induced platelet aggregation and vascular thrombosis. *Brit. J. Pharmacol.* 146(6), 882–893 (2005).

25 Singh SK, Singh MK, Nayak MK *et al.* Thrombus inducing property of atomically thin graphene oxide sheets. *ACS Nano* 5(6), 4987–4996 (2011).

26 Shrivastava S, Bera T, Singh SK *et al.* Characterization of antiplatelet properties of silver nanoparticles. *ACS Nano* 3(6), 1357–1364 (2009).

27 Bass D, Olbrantz P, Szejda P, Seeds M, McCall C. Subpopulations of neutrophils with increased oxidative product formation in blood of patients with infection. *J. Immunol.* 136(3), 860–866 (1986).

28 560CA aggregometer, package insert. Chrono-log Corporation, PA, USA.

29 Chithrani B, Ghazani A, Chan W. Determining the size and shape dependence of gold nanoparticle uptake into mammalian cells. *Nano Lett.* 6(4), 662–668 (2006).

30 Rothen-Rutishauder B, Schürch S, Haenni B, Kapp N, Gehr P. Interaction of fina particles and nanoparticles with red blood cells visualized with advanced microscopic techiques. *Environ. Sci. Technol.* 40(14), 4553–4359 (2006).

31 Bhattacharya R, Patra C, Verma R, Kumar S, Greipp P, Mukherjee P. Gold nanoparticles inhibit the proliferation of multiple myeloma cells. *Adv. Mat.* 19(5), 711–716 (2007).

32 Lundqvist M, Stigler J, Elia G *et al.* Nanoparticle size and surface properties determine the protein corona with possible implications for biological impacts. *Proc. Natl Acad. Sci. USA* 105(38), 14265–14270 (2008).

33 Monopoli M, Walczyk D, Campbell A *et al.* Physical–chemical aspects of protein corona: relevance to *in vitro* and *in vivo* biological impacts of nanoparticles. *J. Am. Chem. Soc.* 133(8), 2525–2534 (2011).

34 Maiorano G, Sabella S, Sorce B *et al.* Effects of cell culture media on the dynamic formation of protein–nanoparticle complexes and influence on the cellular response. *ACS Nano* 4(12), 7481–7491 (2010).

35 De Paoli Lacerda S, Park J, Meuse C *et al.* Interaction of gold nanoparticles with common human blood proteins. *ACS Nano* 4(1), 365–379 (2010).

36 Schaeublin N, Braydich-Stolle L, Schrand A *et al.* Surface charge of gold nanoparticles mediates mechanism of toxicity. *Nanoscale* 3(2), 410–420 (2011).

37 Barathmanikanth S, Kalishwaralal K, Sriram M *et al.* Anti-oxidant effect of gold nanoparticles restrains hyperglycemic conditions in diabetic mice. *J. Nanobiotechnology* 8, 16 (2010).

38 Chompoosor A, Saha K, Ghosh P *et al.* The role of surface functionality on acute cytotoxicity, ROS generation and DNA damage by cationic gold nanoparticles. *Small* 6(20), 2246–2249 (2010).

39 Pan Y, Leifert A, Ruau D *et al.* Gold nanoparticles of diameter 1.4 nm trigger necrosis by oxidative stress and mitochondrial damage. *Small* 5(18), 2067–2076 (2009).

40 Dobrovolskaia M, Patri A, Zheng J *et al.* interaction of colloidal gold nanoparticles with human blood: effects on particle size and analysis of plasma protein binding profiles. *Nanomedicine* 5(2), 106–117 (2009).

41 AshaRani PV, Low Kah Mun G, Hande MP, Valiyaveettil S. Cytotoxicity and genotoxicity of silver nanoparticles in human cells. *ACS Nano* 3(2), 279–290 (2009).

Website

101 Project on emerging nanotechnologies: inventory of nanotechnology consumer products. www.nanotechproject.org/inventories/consumer